KINETICS, CATALYSIS, AND REACTION ENGINEERING

Residence Time Distribution in the Liquid Phase in a Cocurrent Gas−Liquid Trickle Bed Reactor[†]

Dick Stegeman, F. Edwin van Rooijen, Arnoud A. Kamperman, Sjoerd Weijer, and K. Roel Westerterp*

Chemical Reaction Engineering Laboratories, Department of Chemical Engineering, Twente University of Technology, P.O. Box 217, 7500 AE Enschede, The Netherlands

The liquid residence time distribution has been evaluated in a trickle bed reactor applying maximum liquid and gas velocities of respectively 10 and 140 mm·s^{-1}. The influence of the liquid viscosity has been studied, using the piston flow with axial dispersion and mass exchange (PDE) model to evaluate the experiments. The residence time of the liquid phase could be well correlated to the liquid Reynolds and a modified Galileo numbers. The fraction stagnant liquid holdup as determined using the PDE model is less than half the value found from draining experiments and stays constant with increasing liquid velocity for water, while it increases for the more viscous liquid. The Bodenstein number in the dynamic zone coincides with single phase flow. For water the NTU between the dynamic and the stagnant zone is about 0.4, while for the viscous liquid it increases gradually to 2.5 with increasing liquid velocity.

Introduction

A gas−liquid trickle bed reactor is a packed-bed reactor in which the liquid phase flows downward through the reactor. The gas phase can flow either counter- or cocurrently. Because flooding may occur in a countercurrent column, cocurrent flow is preferred if high loads are desired, see Wammes et al. (1991a). At low gas and liquid loads the liquid flows in trickle flow, while at higher gas and liquid flow the pulse flow regime prevails. At elevated pressures the transition between trickle flow and pulse flow shifts toward higher gas and liquid loads; see Wammes et al. (1991b,c). Because nearly all industrial trickle bed reactors operate at elevated pressures, they ordinarily operate in the trickle flow regime.

Although often the liquid phase is said to be in plug flow, this is not necessarily true. Usually the phase can be separated in two different zones; see, for example, Van Swaaij et al. (1969): the dynamic or flow-through zone and the stagnant zone. For trickle bed reactors RTD or *R*esidence *T*ime *D*istribution curves always show slight asymmetric behavior called "tailing". Deviation from plug flow may lead to bad product qualities due to differences in conversion and selectivity. In extreme cases also thermal runaway may occur because of consecutive or side reactions in the stagnant zone. Therefore, it is important to have a good description of the liquid flow through the reactor so process parameters may be changed to reach better product specifications. In this study conductivity measurements have been performed to give a description of the RTD of the liquid phase.

In the last decades different models have been developed to describe the liquid flow in a trickle bed reactor. Some of these models are given by Shah (1979), Gianetto and Berrutti (1986), and Kan and Greenfield (1983). Models like the "dispersed plug flow model" try to describe deviations from plug flow by introducing an
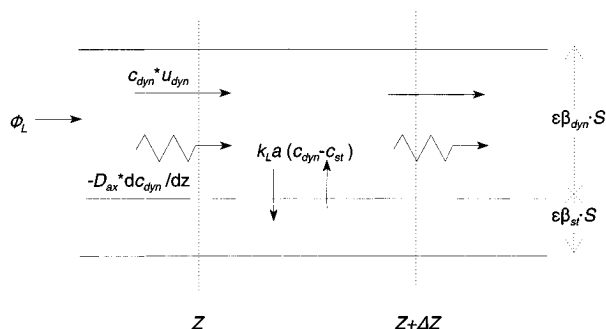

Figure 1. Model of axially dispersed plug flow and mass exchange with dead zones.

axial dispersion coefficient. Although the main part of measured RTD curves can be described well with such a model, tailing of the RTD curve is always underestimated, as is shown by Michell and Furzer (1972), Matsuura et al. (1976), and Yang et al. (1990). The models that correspond best with reality are models that also divide the liquid phase in a dynamic and a stagnant zone, e.g., "the PDE model" with *P*iston flow with axial *D*ispersion and mass *E*xchange between the dynamic and the stagnant zone, of Van Swaaij et al. (1969).

Here the RTD of the liquid phase is described by means of this PDE model. The influence of the liquid viscosity and of the gas and liquid velocity on the different model parameters will also be studied.

Theory

Description of the PDE Model. At approximately the same time Van Swaaij et al. (1969) and Bennett and Goodridge (1970) introduced the PDE model. The model is shown schematically and in the form of equations in respectively Figure 1 and eqs 1 and 2.

$$\frac{\partial C_{dyn}}{\partial x} + \varphi \frac{\partial C_{dyn}}{\partial \theta} + \mathrm{NTU}(C_{dyn} - C_{st}) = \frac{1}{Pe}\frac{\partial^2 C_{dyn}}{\partial x^2} \quad (1)$$

$$\frac{\partial C_{st}}{\partial \theta} + \frac{\mathrm{NTU}}{1 - \varphi}(C_{st} - C_{dyn}) = 0 \quad (2)$$

For the initial conditions $\theta = 0$, $C_{dyn} = C_{st} = 0$, and the

---

Table 1. Comparison between the Residual Holdup Found by Wammes et al. (1991c) and Literature Correlations

liquid	$E\ddot{o}$	$\epsilon\beta_{res}$	$\epsilon\beta_{res}$	$\epsilon\beta_{res}$
		Wammes et al.	eq 4	eq 5
water	1.23	0.05	0.047	0.049
40% ethylene glycol/water	1.55	0.042	0.047	0.043
ethanol	3.17	0.038	0.043	0.026

following boundary conditions for a pulse injection:

$$x = 0 \qquad \delta(\theta) = C_{dyn} - \frac{1}{Pe}\frac{\partial C_{dyn}}{\partial x} \qquad (3)$$

$$x \rightarrow \infty \qquad C_{dyn}, \ C_{st} \rightarrow 0$$

the solution of this system is given by Villermaux and Van Swaaij (1969) and can among others be found in Shah (1979), Mills and Duduković (1989), and Greenfield and Sudarmana (1986).

Liquid Holdup. The liquid holdup can be divided into a dynamic and a stagnant holdup, β_{dyn} and β_{st} respectively. Also another subdivision can be made. If the liquid and gas supply to a trickle bed reactor are stopped suddenly, a part of the liquid holdup will trickle out of the reactor, while another part will stay in the column because of capillary forces. The first part is called the free-draining holdup, β_{fd}, while the second is

referred to as the residual holdup, β_{res}. Although in a part of the literature the residual holdup is also called the stagnant holdup, one should not confuse these two. The stagnant fraction is affected by the process conditions, whereas the residual fraction depends only on the physical properties of the liquid phase and the packing. Under normal process conditions the stagnant holdup is always smaller than the residual holdup because of eddies formed in and around the dead regions.

In literature some relations have been derived for the residual holdup; see Sáez and Carbonell (1985, 1990). Despite their theoretical basis, these relations are not able to give a good description of experimentally determined values of the residual holdup, see Sáez et al. (1991). Van Swaaij et al. (1969) have empirically correlated this residual holdup as a function of the Eötvos number:

$$\epsilon\beta_{res} = \frac{0.05}{1 + 0.045E\ddot{o}} \qquad (4)$$

Sáez et al. (1991) have done experiments with Eötvos numbers between 0.03 and 5 and state eq 4 underestimates the holdup at low Eötvos numbers. Their correlation gives

$$\epsilon\beta_{res} = \frac{0.11}{1 + E\ddot{o}} \qquad (5)$$

Wammes et al. (1991c) have determined the static

Table 2. Empirical Correlations for the Free-Draining and Total Liquid Holdup Found in the Literature

Satterfield and Way (1972)	$0.02 < Re_L < 7.1$ $0 < u_G < 2.3 \ cm\cdot s^{-1}$	$\beta_{fd} = Au_L^{1/3}\eta_L^{1/4} + B$	(6)
Goto and Smith (1975)	$0.3 < Re_L < 16$ $0 < u_G < 0.8 \ cm\cdot s^{-1}$	$\beta_{fd} = Au_L^{1/3}\eta_L^{1/4}$	(7)
Specchia and Baldi (1977)	$0.3 < Re_L < 3000$ $0 \leq u_G \leq 1.1 \ m\cdot s^{-1}$	$\beta_{fd} = 3.86 Re_L^{0.545}\left(Ga_L\left(1 + \frac{\Delta P}{\varrho_L gL}\right)\right)^{-0.42}\left(\frac{a_v d_p}{\epsilon}\right)^{0.65}$	(8)
Kohler and Richarz (1985)	$0.1 < Re_L < 8, \ Re_G = 0$	$\beta_{fd} = 3.42 Re_L^{0.53}Ga_L^{-0.42}\left(\frac{a_v d_p}{\epsilon}\right)^{0.65}$	(9)
	$0.1 < Re_L < 8, \ Re_G < 10$ $0.1 < P < 1.0 \ MPa$	$\beta_{fd} = 0.71\frac{Re_L^{0.53}}{Re_G^{0.31}}Ga_L^{-0.42}\left(\frac{a_v d_p}{\epsilon}\right)^{0.65}$	(10)
Sáez and Carbonell (1985)	$0.2 < Re_L^* < 2000$	$\beta_{fd} = \left(A\frac{Re_L^*}{Ga_L^*} + B\frac{Re_L^{*2}}{Ga_L^*}\right)^{0.41}$	(11)
	$5 \leq Re_L^* \leq 1500$ $5 \leq Re_G^* \leq 6000$	$\frac{1}{\beta_{fd}^{2.43}}\left(A\frac{Re_L^*}{Ga_L^*} + B\frac{Re_L^{*2}}{Ga_L^*}\right) - \frac{\varrho_G}{\varrho_L}\frac{1}{(\epsilon(1 - \beta_{tot}))^{4.8}}\left(A\frac{Re_G^*}{Ga_G^*} + B\frac{Re_G^{*2}}{Ga_G^*}\right) = 1$	(12)
Larachi et al. (1991)	$0.5 < Re_L < 49$ $0.003 < \varrho_G u_G < 2.2 \ kg\cdot m^{-2}\cdot s^{-1}$	$\beta_{tot} = 1 - 10^{-\Gamma}; \ \Gamma = 1.22\frac{We_L^{0.15}}{X_g^{0.15}Re_L^{0.20}}$	(13)
Wammes et al. (1991b,c)	$0 < Re_L < 11, \ u_G = 0 \ m\cdot s^{-1}$ $\alpha = 0.36, \gamma = -0.39$	$\beta_{fd} = 3.8 Re_L^{\alpha}Ga_L^{\gamma}\left(\frac{a_v d_p}{\epsilon}\right)^{0.65}$	(14)
	$2 < Re_L < 55, \ 0 < \varrho_G u_G < 25 \ kg\cdot m^{-2}\cdot s^{-1}$ $\alpha = 0.55, \gamma = -0.42$	$\beta_{fd} = 3.8 Re_L^{\alpha}\left(Ga_L\left(1 + \frac{\Delta P}{\varrho_L gL}\right)\right)^{\gamma}\left(\frac{a_v d_p}{\epsilon}\right)^{0.65}$	(15)
Holub et al. (1993)	$0 < Re_L^* < 150$ $0 \leq Re_G^* < 1000$	$\Psi_L = \left(\frac{1}{\beta_{tot}}\right)^3\left(E_1\frac{Re_L^*}{Ga_L^*} + E_2\frac{Re_L^{*2}}{Ga_L^*}\right)$ $\Psi_G = \left(\frac{1}{1 - \beta_{tot}}\right)^3\left(E_1\frac{Re_G^*}{Ga_G^*} + E_2\frac{Re_G^{*2}}{Ga_G^*}\right)$	(16)

holdup for water, ethanol, and a 40% ethylene glycol−water mixture in a trickle bed reactor packed with 3 mm glass beads. They have shown that relation 4 can give a good description of their determined stagnant holdup. After recalculating their results, it is shown that eq 5 also gives a good estimate of the residual holdup. The relations of Van Swaaij et al. and Sáez et al. show similar errors in the range $1.2 < E\ddot{o} < 3.2$; see Table 1.

For the free-draining holdup in the trickle-flow regime several empirical correlations are known in literature, see Table 2. At low gas flows no influence of the gas flow on the liquid holdup has been found. Studies performed with higher gas mass fluxes revealed a negative influence of the gas flux on the liquid holdup. Frequently the holdup is correlated using the Reynolds number Re and the Galileo number Ga. The Galileo number represents the ratio of Re^2 and the Froude number, $Fr = \rho_L u^2 / d_p \rho_L g$, the ratio between the forces associated with kinetic energy and the forces associated with the acceleration. The pressure difference over the reactor also acts on the liquid phase, so for higher gas loads the Galileo number might have to be corrected for this extra force, e.g., eq 8 in Table 2. Given correlations of the holdup are either by means of a power law or an Ergun-like relation. Specchia and Baldi (1977), Kohler and Richarz (1985), and Wammes et al. (1991b,c) have used a power law, whereas Sáez and Carbonell (1985) and Holub et al. (1993) have modified the Ergun equation to account for a second flowing phase. Because the pressure drop depends among others on the total void fraction in the bed, the Ergun equation implicitly also can be used to correlate the liquid holdup in two-phase flow.

Rewriting the set of eqs 16 in Table 2 of Holub et al. gives a direct correlation between the total liquid holdup and the process parameters:

$$\beta_{tot}{}^3 = \left(E_1 \frac{Re_L{}^*}{\left(1 + \frac{\Delta P}{\varrho_L g L}\right) Ga_L{}^*} + E_2 \frac{Re_L{}^{*2}}{\left(1 + \frac{\Delta P}{\varrho_L g L}\right) Ga_L{}^*} \right) \tag{17}$$

Like in the original Ergun equation, here also a laminar term and a turbulent term are present.

Experimental Apparatus and Procedure

Experimental System. In Figure 2 a simplified flow diagram of the experimental installation is presented. The column is manufactured in plexiglass while the other parts are made of stainless steel 316. The maximum superficial liquid and gas velocities based on the empty reactor cross section are 10 and 140 mm·s^{-1}, respectively. The gas phase used was 99.9 vol % nitrogen. The liquid phase was either deionized water or a mixture of deionized water and 13.5 mol % ETG (ethylene glycol). For the physical constants of the liquid phase, see Table 3.

Reactor System. The reactor has an inner diameter of 54 mm and a total height of 1.1 m. It was filled with 3 ± 0.5 mm glass beads. The total height of the packing was 0.98 m, and the void fraction was measured to be 0.39. The liquid was stored in a 60 L supply vessel equipped with a stirrer. Via the jacket the vessel was thermostated at 25 °C. It was kept under a nitrogen pressure of 3 bar gauge, so the liquid could be transported from vessel to column by pressure difference. The
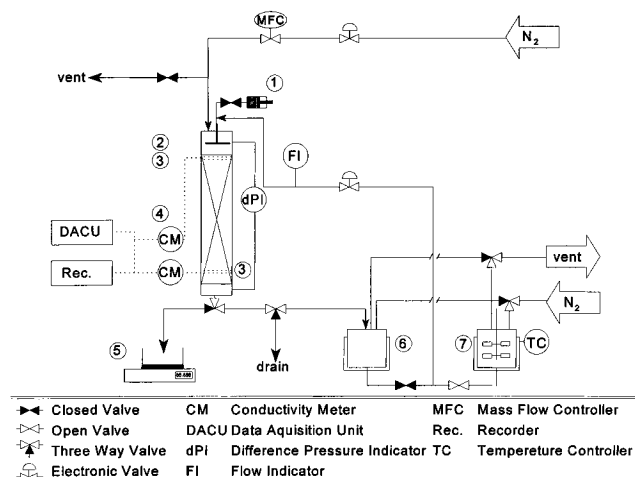

	Closed Valve	CM	Conductivity Meter	MFC	Mass Flow Controller
	Open Valve	DACU	Data Aquisition Unit	Rec.	Recorder
	Three Way Valve	dPi	Difference Pressure Indicator	TC	Tempereture Controller
	Electronic Valve	FI	Flow Indicator		

Figure 2. Experimental setup used: 1, injection plunger; 2, liquid distributor; 3, conductivity cell; 4, packed bed; 5, balance; 6, storage vessel; 7, supply vessel.

Table 3. Physical Properties of the Used Liquid Phases

	deionized water	water/ETG mixture
x_w	1	0.865 mol of water/mol of mixture
ρ_L	1000 kg·m^{-3}	1041 kg·m^{-3}
η_L	0.0010 Pa·s	0.0021 Pa·s
σ	0.072 N·m^{-1}	0.062 N·m^{-1}

liquid flow was measured with a rotameter and uniformly spread over the packing by a liquid distributor with nine holes of 0.4 mm. The gas was taken from bottles, and its velocity was measured with a mass flow controller. It was possible to open and close the gas and liquid inlets by electronic valves. The bottom of the column was kept at ambient pressure.

Conductivity Measurement. Conductivity measurements were performed to determine the RTD curves. As tracer we used a KBr solution of 200 g/L either in deionized water or in a mixture of water and ETG. It was injected as a pulse in the liquid distributor by a pneumatic injection plunger. A δ-Dirac pulse could be well approximated. For a full description of the injection system, see Van Gelder and Westerterp (1990). A conductivity cell was placed in the top of the reactor to check the pulse injection. The other cell was placed 5 cm above the bottom of the packed bed. The cells were made of two round SS 316 gauzes with a mess of 5 mm and placed at a distance of 4 mm apart so the packing particles could fit well in the cell. Moreover, this way the cell was totally integrated in the bed. The data were gathered by a computer via two conductivity meters.

Liquid Holdup. To ensure reproducibility, the column was totally wetted by closing the outlet, filling the reactor with liquid, and draining the whole column. This procedure was repeated three times before the start of a measurement. Then the required gas and liquid velocities were set, and the column was stabilized for about 15 min. After that, the gas and liquid inlet flows were stopped suddenly and simultaneously by two electronic valves, whereas the outlet flow was redirected to a liquid collector. To account for inlet and outlet phenomena, the measurements were performed for two column heights. The total free-draining holdup was taken as the difference of these two series.

The residual holdup was measured in a separate column. The holdup was calculated by the difference in weight of a dry column and of the same column after it was flushed with liquid. Here the column was totally filled with liquid and drained slowly; no gas phase was

Table 4. Comparison between the Experimental Liquid Holdup and the Given Relations (MSD = Mean Standard Deviation; MD = Mean Deviation)

ref	eq no.	MSD	MD
Specchia and Baldi	8	0.047	0.040
Kohler and Richarz	9	0.23	0.21
Sáez and Carbonell	11	0.11	0.092
Sáez and Carbonell	12	0.16	0.15
Larachi et al.	13	0.36	0.36
Wammes et al.	14	0.048	0.041
Holub et al.	16	0.12	0.10
only correlating β_{fd}	19	0.022	0.017

Figure 3. Comparison between the residence time calculated from the total liquid holdup and the first moment of the measured RTD curve.

introduced. The total liquid holdup and the liquid volume flux were used to calculate the mean residence time τ_β.

RTD Measurement. For the RTD measurements the same procedure of wetting was used as for the determination of the free-draining holdup. The top conductivity cell was only used to inspect whether the tracer was injected as a correct pulse. The gathered conductivity data were converted to RTD curves by normalizing the data and smoothing the curves by a 17-point mathematical filter; see Savitsky and Golay (1964). The residence time τ is calculated as the first moment of the $E(t)$ curves. The RTD curves were converted to dimensionless $E(\theta)$ curves with the first moment of the $E(t)$ curve. All experiments were performed in 3-fold. The $E(t)$ versus t curves and τ were used to check the reproducibility of the experiments.

At least 30 points of the dimensionless curves were used to fit model curves to the experimental curves. These points were always taken in a way that one-third of the points was in the tail of the curves and two-thirds of the points were taken from the rest of the $E(\theta)$ curves. The maximal $E(\theta)$ value always made part of these points. The best fitting parameter values were found by minimizing a relative target function:

$$F_{rel} = \frac{\displaystyle\sum_{i=1}^{n} \frac{abs(E(\theta)_{i,e} - E(\theta)_{i,m})}{E(\theta)_{i,m}}}{n} \qquad (18)$$

The relative target function assigns equal importance to the entire RTD curve, so it also takes the tail into account.

Results

Liquid Holdup. At low rates, the gas flow does not influence and at higher velocities it does diminish the liquid holdup. Thus, for correlating the liquid holdup also the gas velocity has to be considered. The best relations to describe our measurements are the relations given by Specchia and Baldi (1977) and Wammes et al. (1991b,c) (respectively eqs 8 and 15). In Table 4 the mean standard deviation (MSD) and the mean deviation (MD) are given. Here we have set the constants A and B in eq 11 to respectively 180 and 1.8 as advised by Sáez and Carbonell. E_1 and E_2 in eq 17 were set at 150 and 1.75, respectively.

The modified Ergun equation (eq 17) is intended to describe the total liquid holdup. Because of the underlying assumption that capillary forces can be ignored, it will not give a very good description of the total liquid holdup. As a result of these capillary forces, a part of the liquid remains stagnant, also under flow conditions, so eq 17 will underesti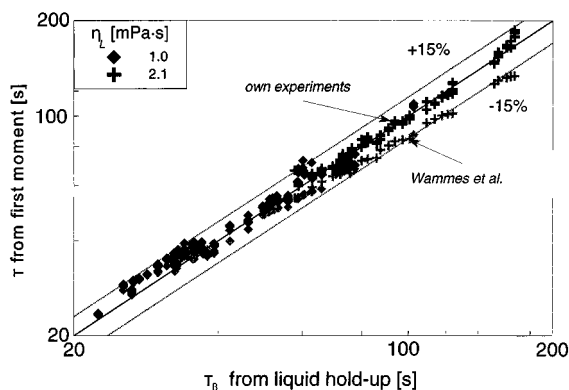mate the total liquid holdup at low liquid velocities if the original Ergun constants are used. However, eq 17 could give a rather good prediction of the free-draining holdup if the constants were a little altered; see Table 4. Because we have not reached the turbulent region, only the laminar term is of importance, and the turbulent term can be set equal to zero. Our data could best be described with:

$$\beta_{fd}{}^3 = 140 \frac{Re_L{}^*}{Ga_L{}^*\left(1 + \dfrac{\Delta P}{\varrho_L g L}\right)} \qquad (19)$$

The value of 140 only differs a little from the original value $E_1 = 150$ given by Ergun (1952). So for laminar flow the modified Ergun correlation is suitable to give a good first approximation of the free-draining holdup; this is not so of the total liquid holdup.

Results of the RTD Measurements. Tailing can play an important role in the calculation of the first moments of the RTD curves and in the shape of the dimensionless $E(\theta)$ curves. We have made a comparison between these first moments, τ, and the residence time τ_β calculated from the liquid holdup, as described earlier. In Figure 3 the residence time values from the total liquid holdup for both liquids are plotted with solid black symbols versus the values of the first moments: it can be seen that almost all first moments are equal to the residence times calculated from the liquid holdup. So the tail of the measured curves correctly has been taken into account.

Wammes et al. (1991b) also derived a correlation to estimate the pressure drop in a trickle bed reactor:

$$\frac{\Delta P}{1/2 \varrho_G V_G{}^2}\left(\frac{d_p}{L}\right) = 155\left(\frac{\varrho_G V_G \epsilon d_p}{\eta_G(1-\epsilon)}\right)^{-0.37}\left(\frac{1-\epsilon}{\epsilon(1-\beta_{tot})}\right) \qquad (20)$$

This relation is obtained at elevated pressures with gas flow, and the authors state that the relation is valid for $\rho_G v_G d_p \epsilon / \eta_G (1-\epsilon) > 200$. We also have tested the applicability of this relation together with the relations for the free-draining holdup (eq 15 in Table 2) and the stagnant holdup (eq 4) for our setup. The calculated values for the residence time using the correlations of Wammes et al. are plotted in Figure 3 with gray symbols. It can be seen it is possible to estimate the total liquid holdup, and thus the mean residence time, at atmospherical conditions within reasonable accuracy using the relations proposed by Wammes et al. Only at low gas and liquid velocities the values for τ are underestimated with 15% or even more.
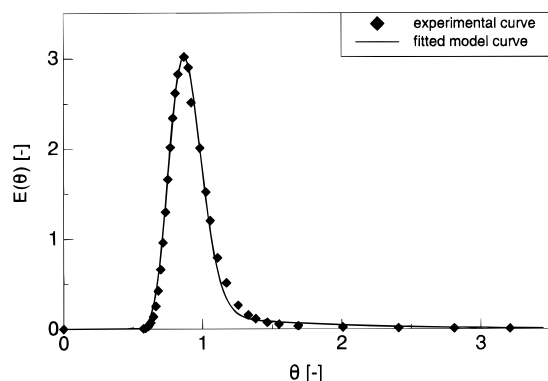
Figure 4. Comparison between the measured RTD curve and the model curve with the best-fit parameters.
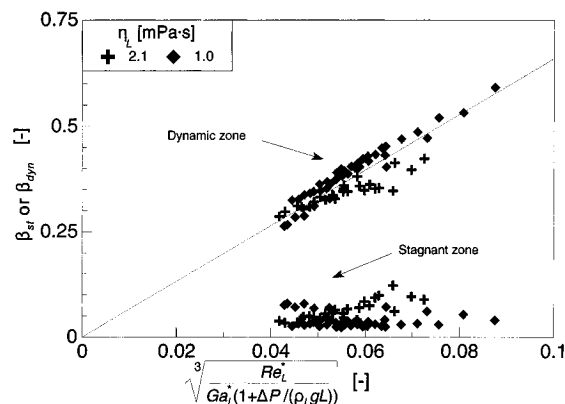

Figure 5. Stagnant and dynamic liquid holdup as a function of the modified laminar term of the Ergun equation.

With the fitted parameters the model gives a good description of the measured RTD curves. In Figure 4 a typical example is given.

Determination of the Model Parameters. Sensitivity of the Model Parameters. Because the PDE model, the first moment not included, consists of three model parameters which may lead to cross-relations between the different parameters, we have studied the model and its sensitivity toward the parameters in more detail. From this study it was concluded that there is no cross-correlation between the parameters mutually, but Pe and NTU especially are very sensitive toward deviations of the first moment. This sensitivity is more pronounced for an underestimation of the first moment than for an overestimation.

Fraction Dynamic Volume. To examine the liquid phase more precisely, the values for the stagnant and dynamic holdup are derived from the total liquid holdup and φ values determined. Like the total free-draining holdup, we have correlated the values of β_{st} and β_{fd} like was done in eq 19. We have varied the dimensionless pressure drop $\Delta P/\rho_L gL$ between 0 and 1.2 in our work. By correcting the Galileo number for the pressure drop also the influence of the gas velocity indirectly is included.

In Figure 5 these parameters are plotted as a function of the cubic root of the modified Reynolds over the Galileo number. From this figure we can observe that for water the stagnant liquid holdup is hardly affected by the term $[Re_L{}^*/Ga_L{}^*(1 + \Delta P/\rho_L gL)]^{1/3}$, while the dynamic liquid holdup increases almost linearly with this group. In the figure also the line for $\beta = 6.6[Re_L{}^*/Ga_L{}^*(1 + \Delta P/\rho_L gL)]^{1/3}$ is drawn. This line gives a good description of the dynamic holdup in water. The dynamic holdup for the liquid with $\eta_L = 2.1$ mPa·s
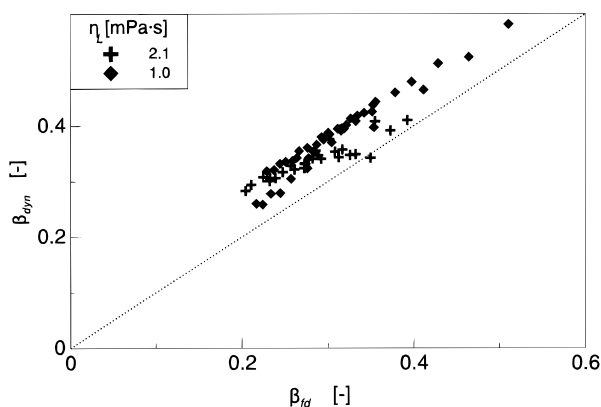

Figure 6. Parity plot between the free-draining holdup and the dynamic liquid holdup.

follows the line for low values of β_{dyn}, while it deviates for larger holdup values. For $\eta_L = 2.1$ mPa·s the stagnant liquid holdup also seems to increase with increasing Reynolds numbers. For both liquids the stagnant liquid holdup in the experimental range is lower than the residual holdup, which is about 0.12. For the more viscous liquid the value of β_{st} is close to the value of β_{res} for high Reynolds numbers.

This discrepancy between the results of the two liquids may be explained by the difference in liquid flow. An increase of the liquid velocity has two effects. First, it will increase the total liquid holdup, leading to an increase in the dynamic holdup. Second, the more intense turbulence in the dynamic zone should decrease the stagnant fraction. Probably for water the second effect levels out the first effect completely, while for $\eta_L = 2.1$ mPa·s the first effect is more pronounced. Maybe the liquid film increases not only in thickness but also in size, because the wetting increases and the packing area is better utilized. We observed at the higher viscosity that the liquid flows more in rivulets, while at the lower viscosity the liquid forms a real film over the packing particles.

To compare the dynamic holdup with the free-draining holdup, we have plotted both holdup values in a parity plot; see Figure 6. It shows that β_{dyn} is always larger than β_{fd}, and for water this difference is almost constant and about 0.07 in the experimental range. For the more viscous liquid it shows more scatter, and the values of β_{dyn} and β_{fd} are reaching almost the same value for larger values of β_{dyn}, while at smaller liquid velocities the difference also is about 0.07. As β_{res} is around 0.12, we may say that only around 40% of the residual holdup acts as a real dead zone for signal processing. So although a larger part of the liquid phase is strongly affected by capillary forces, there is still a high interaction between the free-draining holdup and the residual holdup. About 60% of the residual holdup is in full motion for mass transfer of signal material in the main part of our experimental range.

Axial Dispersion in the Dynamic Zone. Using the dimensionless Navier–Stokes equation for a steady vertical film flow in a conduit, it follows that

$$\frac{\partial^2 U}{\partial X^2} + \frac{\partial^2 U}{\partial Y^2} \propto -\left(\frac{Re}{Fr}\right) \qquad (21)$$

in which X and Y are the dimensionless Cartesian coordinates perpendicular to the flow direction and U is the dimensionless film velocity. Assuming that a pressure difference over the reactor only has an impact
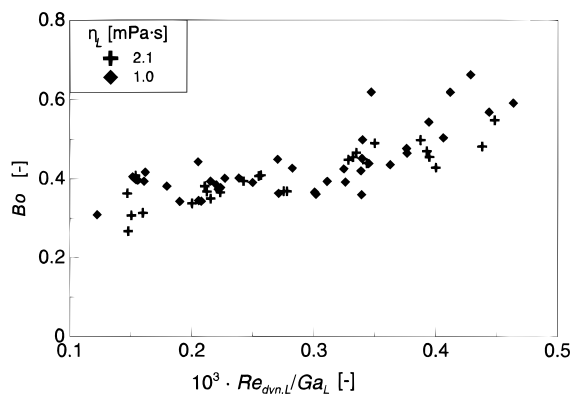
Figure 7. Bodenstein number for the dynamic liquid phase versus the Reynolds number based on the dynamic liquid velocity over the Galileo number.

Figure 8. Mass transfer between the dynamic and stagnant zones versus the Reynolds number based on the dynamic liquid velocity over the Galileo number.

on the size of the liquid holdup and not on the mixing in the liquid phase, we take that it is appropriate to describe the mixing parameters as a function of the Reynolds and the Froude number. Here the Reynolds number should be defined on the dynamic liquid velocity. As the characteristic length the sphere diameter is taken. To present our results consistently with the previous ones, Re/Ga (=Fr/Re) is used instead of Re/Fr. The dimensionless group Re/Ga represents the viscous forces over the gravity forces.

To describe the axial dispersion in the dynamic zone, the Péclet number is rewritten into a Bodenstein number, based on the particle diameter:

$$Bo = Pe(d_p/L) \qquad (22)$$

In Figure 7 a plot is given of the values determined for the Bodenstein number versus $Re_{dyn,L}/Ga_L$; there is no systematic difference between the two data sets for the two different viscosities. Further a theoretical evaluation would predict the film thickness is proportional to $\beta_{dyn}d_p$. As Bo increases 2-fold between $0.1 \times 10^{-3} < Re_{dyn,L}/Ga_L < 0.4 \times 10^{-3}$, we may assume that the increase is caused by both better wetting and increasing film thickness. The values of the Bodenstein number are in the range between 0.3 and 0.65 for both liquids. For $Re_{dyn,L}/Ga_L \leq 0.3 \times 10^{-3}$ the Bodenstein number is almost constant, and for larger values it starts to increase gradually. At $Re_{dyn,L}/Ga_L = 0.3 \times 10^{-3}$ the corresponding Reynolds numbers in the dynamic zone are 80 and 20 respectively for $\eta_L = 1$ and 2.1 mPa·s. The values of the Bodenstein number agree with the ones found for single-phase liquid flow in packed beds, see Westerterp et al. (1984). Bodenstein numbers below 0.5 indicate a higher level of dispersion in the dynamic zone than in the case where all the void volume was occupied by the liquid.

Mass Transfer between the Dynamic Zone and the Stagnant Zone. In the PDE model the number of transfer units is proportional to a mass-transfer coefficient k_L, times the interfacial area between the dynamic and stagnant fraction of the holdup a, defined per unit of total reactor volume. For water the number of mass-transfer units between the dynamic and the stagnant regions is about 0.4 for our column, while for the more viscous liquid the number increases with increasing liquid velocity and even reaches a value of 2.5. We have rewritten the number of mass-transfer units to the mass-transfer coefficient:

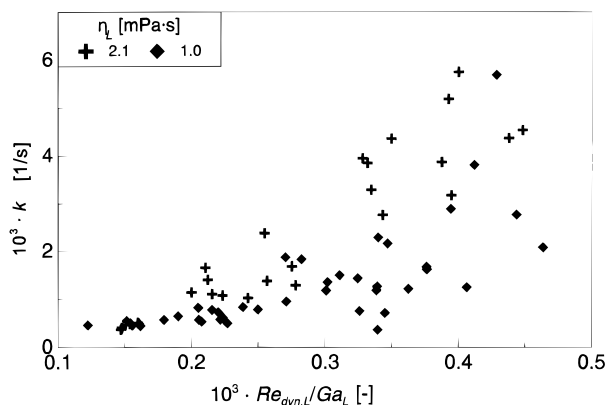$$k = k_L a = u_L NTU/L \qquad (23)$$

In Figure 8 we have plotted the $k_L a$ values as a function of the dynamic Reynolds over the Galileo number. All values are in the range between 0.0002 and 0.006 s^{-1}. Although the figure shows a large scatter, we can observe that the mass-transfer coefficient increases constantly with increasing liquid Reynolds numbers. For the more viscous liquid the increase is more pronounced than for the less viscous one.

Discussion and Conclusions

The liquid residence time distribution in a trickle bed reactor has been evaluated using the PDE model. The model gives a good description of the measured RTD curves. The optimized parameter values show a large scatter. Several factors play an important role in the indetermination. The first factor is the measurement itself. A trickle bed reactor is a dynamic system, and stream lines in the reactor change constantly in time. Placing the conductivity cell inside the packed bed—so without need of any adaption of the measured data for unknown mixing inside the measuring compartment—has the disadvantage that the liquid flow through the cell also ever changes. This may change the conductivity measured in the cell. Further the measured conductivity of the carrier liquid may change in time during an experiment. A change in conductivity above all affects the shape of the tail. Although first moments are comparably large to the ones found from the liquid holdup measurements, this effect in the tail will have its influence on the fitted parameters.

The second factor is the model itself. A model with four parameters can easier give a good fit of the measured data than models having fewer parameters. Small deviations from ideal RTD curves will give rise to scatter in Pe and NTU. Also an underestimation of the residence time, used to transpose the measured curve to a dimensionless curve, will have a great impact on the value of NTU.

For water the dynamic liquid holdup increases with increasing liquid velocity and decreasing gas velocity, while the stagnant holdup stays constant. For the more viscous liquid both holdup values increase with increasing liquid velocity and decreasing gas velocity. Also the mass transfer between the dynamic and stagnant zone increases with the liquid velocity. For the more viscous liquid the mass transfer is larger than for water at the same values of $Re_{dyn,L}/Ga_L$, based on the dynamic liquid velocity. The axial dispersion in the dynamic zone is hardly affected by the gas velocity, whereas it increases

with increasing liquid velocity. The Bodenstein numbers are comparable with values reported for single-phase flow.

We may conclude that model curves give a good fit of the experimental curves, but values of the best-fit parameters are not unique. This is due to an inaccuracy in the determination of the RTD curves and in the model itself. The model has four parameters which can be adapted to give a good fit, with a large scatter of the individual parameter values. Although the average residence times can be determined within 10% accuracy, the deviations in the calculated model parameters are larger.

Acknowledgment

Nomenclature

A = constant in Table 2
a = specific interfacial area between dynamic and stagnant zone, $m^2 \cdot m^{-3}$ of liquid
a_v = geometrical external surface, $m^2 \cdot m^{-3}$ of reactor
B = constant in Table 2
$Bo = u_L d_P / D_{ax}$, Bodenstein number for axial dispersion
C = dimensionless concentration
c = concentration, mol of tracer$\cdot m^{-3}$ of liquid
D_{ax} = dispersion coefficient, $m^2 \cdot s^{-1}$
d_p = particle diameter, m
E_1, E_2 = constant of the Ergun equation for single-phase flow
$E(t)$ = residence time distribution function, s^{-1}
$E(\theta)$ = residence time distribution curve based on the dimensionless time
$E\ddot{o} = \rho_L g d_p^2 / \sigma_L$, Eötvos number
ETG = ethylene glycol
F = target function
$Fr_\alpha = u_\alpha^2 / d_p g$, Froude number of phase α
$Ga_\alpha = \rho_\alpha^2 g d_p^3 / \eta_\alpha^2$, Galileo number of phase α
$Ga_\alpha^* = (\rho_\alpha^2 g d_p^3 / \eta_\alpha^2)[\epsilon^3/(1-\epsilon)^3]$, bed Galileo number of phase α
g = gravitational acceleration constant, $m \cdot s^{-2}$
$k = k_L a$, apparent mass-transfer coefficient, s^{-1}
k_L = mass-transfer coefficient between the zones, $m \cdot s^{-1}$
L = length of the packed bed c.q. measuring section, m
n = number of points
NTU = $k_L a L / u_L$, number of transfer units
P = pressure, Pa
$Pe = u_{dyn} L / D_{ax}$, Péclet number for axial dispersion
$Re_\alpha = r_\alpha u_\alpha d_p / \eta_\alpha$, Reynolds number of phase α, referred to superficial velocity
$Re_\alpha^* = \rho_\alpha u_\alpha d_p / \eta_d (1-\epsilon)$, bed Reynolds number of phase α
$Re_{i,L} = \rho_L u_L d_p / \eta_L \epsilon \beta_{tot}$, Reynolds number of the liquid phase, referred to interstitial velocity
S = cross-sectional area of the reactor, m^2
t = time, s
$U = u/\bar{u}$, dimensionless velocity
u_α = superficial velocity (based on an empty cross section of the reactor), $m \cdot s^{-1}$
u_{dyn} = mean liquid velocity in the dynamic zone, $m \cdot s^{-1}$
$v_G = u_G / (\epsilon (1-\beta_{tot}))$, mean gas velocity, $m \cdot s^{-1}$
$We = L^2 d_p / \rho_L \sigma_L$, Weber number
x = dimensionless axial coordinate
x_w = mole fraction of water, mol of water $\cdot mol^{-1}$ of mixture
z = axial coordinate, m

Greek Symbols

β = liquid holdup fraction in the empty space, m^3 of liquid$\cdot m^{-3}$ of void
Γ = parameter defined in eq 13
$\delta(\theta)$ = Dirac function based on the dimensionless time
ϵ = overall porosity of the packed bed, m^3 of free space$\cdot m^{-3}$ of reactor
η = dynamic viscosity, $Ns \cdot m^{-2}$
θ = dimensionless time, $t \cdot \tau^{-1}$
$\varphi = \beta_{dyn}/(\beta_{dyn} + \beta_{st}) = \beta_{dyn}/\beta_{tot}$, fraction dynamic volume
ρ = density, $kg \cdot m^{-3}$
σ_L = gas−liquid surface tension, $N \cdot m^{-1}$
$\tau_\beta = \epsilon(\beta_{fd} + \beta_{res})LS/\phi_L$, residence time calculated from liquid holdup, s
τ = first moment of the $E(t)$ curve, s
ϕ = flow rate, $m^3 \cdot s^{-1}$
$X_g = (\phi_G/\phi_L)(\rho_L/\rho_G)^{1/2}$, modified Lockhart−Martinelli parameter
$\Psi_\alpha = (\Delta P/L + \rho_\alpha g)/\rho_\alpha g$, dimensionless force acting on phase α

Superscripts and Subscripts

0 = start
abs = absolute
dyn = dynamic zone
e = experimental
fd = free draining
G = gas
L = liquid
m = model
res = residual
rel = relative
st = stagnant zone
α = alpha phase, either gas or liquid

Literature Cited

Bennett, A.; Goodridge, F. Hydrodynamic and Mass Transfer Studies in Packed Absorption Columns, Part I: Axial Liquid Dispersion. *Trans. Inst. Chem. Eng.* **1970**, *48*, T232.

Ergun, S. Fluid Flow through Packed Beds. *Chem. Eng. Prog.* **1952**, *48*, 89.

Gianetto, A.; Berrutti, F. Modelling of Trickle Bed Reactors. In *NATO ASI Series: Chemical reactor design and technology*; de Lasa, H. I., Ed.; Nijhoff: Dordrecht, The Netherlands, 1986; p 631.

Goto, S.; Smith, J. M. Trickle-Bed Reactor Performance. Part 1: Holdup and Mass Transfer Effects. *AIChE J.* **1975**, *21*, 706.

Greenfield, P. F.; Sudarmana, D. In *Encyclopedia of Fluid Mechanics;* Cheremisinoff, M. P., Ed.; Houston Gulf Publishing, Houston, TX, 1986; p 1019.

Holub, R. A.; Duduković, M. P.; Ramachandran, P. A. Pressure Drop, Liquid Holdup, and Flow Regime Transition in Trickle Flow. *AIChE J.* **1993**, *39*, 302.

Kan, K. M.; Greenfield, P. F. A Residence-Time Model for Trickle-Flow Reactors Incorporating Incomplete Mixing in Stagnant Regions. *AIChE J.* **1983**, *29*, 123.

Kohler, M.; Richarz, W. Investigation of Liquid Holdup in Trickle Bed Reactors. *Ger. Chem. Eng.* **1985**, *8*, 295.

Larachi, F.; Laurent, A.; Midoux, N.; Wild, G. Experimental Study of a Trickle-Bed Reactor Operating at High Pressure: Two-Phase Pressure Drop and Liquid Saturation. *Chem. Eng. Sci.* **1991**, *46*, 1233.

Matsuura, A.; Akehata, T.; Shirai, T. Axial Dispersion of Liquid in Concurrent Gas−Liquid Downflow in Packed Beds. *J. Chem. Eng. Jpn.* **1976**, *9*, 294.

Michell, R. W.; Furzer, I. A. Mixing in Trickle Flow through Packed Beds. *Chem. Eng. J.* **1972**, *4*, 53.

Mills, P. L.; Duduković, M. P. Convolution and Deconvolutiuon of Nonideal Tracer Response Data with Application to Three-Phase Packed Beds. *Comput. Chem. Eng.* **1989**, *13*, 881.

Sáez, A. E.; Carbonell, R. G. Hydrodynamic Parameters For Gas−Liquid Cocurrent Flow in Packed Beds. *AIChE J.* **1985**, *31*, 52.

Sáez, A. E.; Carbonell, R. G. The Equilibrium and Stability of Menisci between Touching Spheres under the Effect of Gravity. *J. Colloid Interface Sci.* **1990**, *140*, 408.

Sáez, A. E.; Yépez, M. M.; Cabrera, C.; Soria, E. M. Static Liquid Holdup in Packed Beds of Spherical Particles. *AIChE J.* **1991**, *37*, 1733.

Satterfield, C. N.; Way, P. F. The Role of the Liquid Phase in the Performance of a Trickle Bed Reactor. *AIChE J.* **1972**, *18*, 305.

Savitsky, A.; Golay, M. J. E. Smoothing and Differentiation of Data by Simplified Least Squares Procedures. *Anal. Chem.* **1964**, *36*, 1627.

Shah, Y. T. *Gas−Solid−Liquid Reactor Design*; McGraw-Hill Inc.: New York, 1979.

Specchia, V.; Baldi, G. Pressure Drop and Liquid Holdup for Two Phase Concurrent Flow in Packed Beds. *Chem. Eng. Sci.* **1977**, *32*, 515.

Van Gelder, K. B.; Westerterp, K. R. Residence Time Distribution and Holdup in a Cocurrent Upflow Packed Bed Reactor at Elevated Pressure. *Chem. Eng. Technol.* **1990**, *13*, 27.

Van Swaaij, W. P. M.; Charpentier, J. C.; Villermaux, J. Residence Time Distribution in the Liquid Phase of Trickle Flow in Packed Columns. *Chem. Eng. Sci.* **1969**, *24*, 1083.

Villermaux, J.; Van Swaaij, W. P. M. A representative model for the residence time distribution in a semi-infinite reactor with axially dispersed piston flow and stagnant zones. Application for trickle flow in a column wth Raschig rings. *Chem. Eng. Sci.* **1969**, *24*, 1097.

Wammes, W. J. A.; Middelkamp, J.; Huisman, W. J.; deBaas, C. M.; Westerterp, K. R. Hydrodynamics in a Cocurrent Gas−

Liquid Trickle Bed at Elevated Pressures, Part 1: Gas−Liquid Interfacial Areas. *AIChE J.* **1991a**, *37*, 1849.

Wammes, W. J. A.; Middelkamp, J.; Huisman, W. J.; deBaas, C. M.; Westerterp, K. R. Hydrodynamics in a Cocurrent Gas−Liquid Trickle Bed at Elevated Pressures, Part 2: Liquid Holdup, Pressure Drop, Flow Regimes. *AIChE J.* **1991b**, *37*, 1854.

Wammes, W. J. A.; Mechielsen, S. J.; Westerterp, K. R. The Influence of Pressure on the Liquid Holdup in a Cocurrent Gas-Liquid Trickle−Bed Reactor Operating at Low Gas Velocities. *Chem. Eng. Sci.* **1991c**, *46*, 409.

Westerterp, K. R.; Van Swaaij, W. P. M.; Beenackers, A. A. C. M. *Chemical Reactor Design and Operation*; John Wiley and Sons: Chichester, U.K., 1984.

Yang, X. L.; Euzen, J. P.; Wild, G. Residence Time Distribution of the Liquid in Gas−Liquid Cocurrent Upflow Fixed Bed Reactors with Porous Particles. *Chem. Eng. Sci.* **1990**, *45*, 3311.